Performance Comparison of a Scintillation Detector NaI(TI) and a High-purity Germanium Semiconductor Detector for the Detection of Radioactivity of Environmental Samples

Nikita Sichov - nsichov@ethz.ch
Supervisor: Andreo Crnjac - acrnjac@phys.ethz.ch

December 11, 2025

Contents

Introduction **3**
Theoretical Background . . . 3
Cesium-137 . . . 3
Photoelectric Absorption . . . 3
Compton scattering . . . 4
Pair production . . . 4
Scintillation detector: NaI(TI) . . . 4
Practical Remarks . . . 4
Semiconductor detector: high-purity Germanium . . . 5
Practical Remarks . . . 5
Radioactive Activity . . . 5

Experiment **5**
Calibration . . . 6
Execution . . . 6
Estimation of Source Activity . . . 6
Activity Equation: Scintillation Detector . . . 8
Activity Equation: Semiconductor Detector . . . 9

Results **9**
Gaussian Fit of Photo-Peaks . . . 9
Source Activity . . . 10
First estimation . . . 10
Activity of different Sources . . . 11

Discussion **12**
Graphical Analysis . . . 12
Comparison of Photo-peak Detection . . . 13
Source Activity . . . 14
Different Sources . . . 14
Mixture A and Mixture B . . . 14

Conclusion **15**

Appendix **15**

Abstract

The primary goal of our experiment is to compare the scintillation and the semiconductor detectors in how well they can detect gamma rays of a variety of sources. Gamma rays are photons excited from the nucleus, their massless and chargeless nature makes them difficult to detect meaning the process of detection is done with photons' interaction with electrons. In the experiments, we see that the semiconductor experiment tends to be more precise and more efficient than the scintillation detector, but measuring the activity of the sources proved to be difficult for either devices.

Introduction

Theoretical Background

Gamma rays are high-energy photons produced from a nuclear interaction. This interaction was first discovered by Paul Villard in 1900 (1860-1934) while studying the behaviour of radium and named by Ernest Rutherford (1871-1937) due to its strong penetrative nature.[1] Nonetheless gamma rays can be stopped by lead due to a high electron density.[1]
Gamma rays are emitted when nuclei are energized[2] past a certain threshold. Usually a gamma ray is emitted so as to bring an atom to a more stable state (minimum energy state).

Cesium-137

Cesium-137 is a good example of a typical nuclear reaction producing gamma rays due to it's single, protruding photo-peak of 662 keV. This is excellent for calibration and is typically used for radiation-detection equipment[3], radiation therapy, flow meters, thickness gauges and moisture-density gauges. Cesium-137 has a half-life of about 30 year and it decays by beta emission into barium-137. There are two paths in this decay, one is a beta decay of 0.5120 MeV followed by a gamma decay of 0.6617 MeV or a direct path 1.174 MeV decay as depicted in Figure 1 with the equation (1) where e^- is an electron and $\bar{\nu}_e$ is an antineutrino. This path of decay makes up 85.1% of the total radioactive interactions.[1]

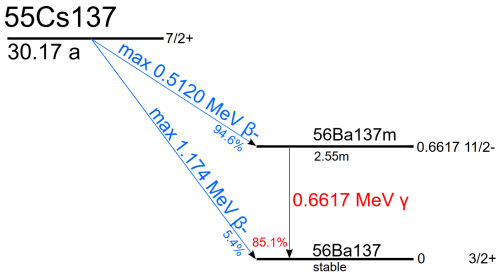

Figure 1: ^{137}Cs decay scheme showing the two radiation paths that are taken, one that emits a gamma ray (85.1%) and one that doesn't (14.9%).

$$^{137}_{55}\mathrm{Cs} \longrightarrow ^{137m}_{56}\mathrm{Ba} + e^- + \bar{\nu}_e \longrightarrow ^{137}_{56}\mathrm{Ba} + \gamma + e^- + \bar{\nu}_e \tag{1}$$

Gamma rays (photons) are difficult to directly measure as they are massless and have no charge, but its interaction with electrons (a subatomic particle with mass and charge) is the core behind the workings of our two detectors. To study this further we must identify three key cases of interaction:

Photoelectric Absorption

A gamma photon is absorbed by an atomic electron, which excites it out of a stable bounded state, releasing it with a kinetic energy equivalent to the incident photon:

$$T = h\nu - E_b \tag{2}$$

[1] Gamma decay is much more penetrative than other forms of decay: Alpha (helium-4 nucleus) and Beta (electron) decay
[2] Energization can happen by a collision or the absorption of photon energy.
[3] We will use Cs-137 clear photo-peak to help calibrate our two detectors.

Where T is the kinetic energy, ν is the photon frequency and E_b is the binding energy.

Compton scattering

A photon strikes an electron causing a momentum conserving interaction where the electron recoils from a rest position. Solving the interaction with energy and momentum conservation gives:

$$h\nu' = \frac{h\nu}{1 + \frac{h\nu}{m_0 c^2}(1 - \cos(\theta)} \tag{3}$$

where ν is the incident photon frequency, m_0 is the rest mass of the electron, θ is the electron's angle of recoil to the incidence and ν' is the scattered photon's frequency. The energy range due to this interaction is a continuum due to the angle dependent nature of the interaction.

Pair production

At high enough energy,[4] a photon can transform into an electron-positron pair.

$$E_{e^-} + E_{e^+} = h\nu - 2m_0 e^2 \tag{4}$$

A second interaction may occur if the released positron interacts with an electron then two annihilation photons[5] are produced. If one of the annihilation photons escape without interaction, it is seen as a "single escape peak" with energy corresponding to the incident photon.

Scintillation detector: NaI(TI)

The thallium-doped sodium iodide detectors (NaI(TI)) responds to gamma photons by scintillation. A ray, from the radioactive source, transfers energy to electrons that are promoted to an excited electron state. Then, it return to the ground state and release the energy as low-energy photons. The low-energy characteristic enable them to freely travel through the scintillator[6] and hit a photocathode at the end of the scintillator. There, a photoelectron is ejected from the surface and this electron is directed towards a photomultiplier made of multiple dynodes. These dynodes, each increasing in potential by $\Delta V \approx 100V$, release more and more low-energy electrons[7] until the cluster of electrons hit the anode. The large number of electrons cause a sharp current pulse which can be detected by an oscilloscope. The schematic of this process is found on Figure 2.

Practical Remarks

In order to not overexpose the experimenter to radiation, the source is put into a thick lead casing which can only emit into the scintillator. The scintillator uses a crystal which is fragile due to its hygroscopic nature[8] therefore it is encased in a moisture-protective casing.

[4] More specifically, pair production occurs when the energy of a photon exceeds 1.02 MeV (twice the rest mass of an electron).

[5] Two photons happen because one would violate momentum conservation. By the same principle the photons emit in opposite directions.

[6] Photons can "travel freely" at low energy because they don't have enough energy to interact with the electrons again.

[7] For each electron that hits a dynode, 5 new ones are re-emitted

[8] Water vapor in the atmosphere is enough to damage the scintillator crystal.

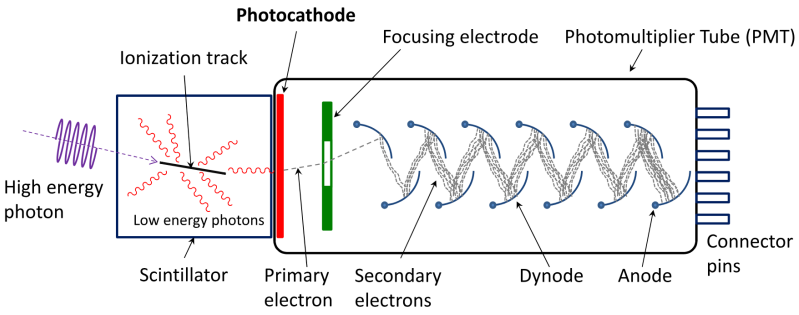

Figure 2: Schematic of the photomultiplier tube with the scintillator. The High energy photon is emitted from the radiation source and the anode the

Semiconductor detector: high-purity Germanium

The allowed energy states of a periodic lattice of a crystalline material are either the valence band or the conduction band. If there is an energy gap between the bands (such as in insulators or semiconductors), effect such as excitations to the electrons may cause valence band electrons to move up to the conduction band and leave a hole in the atom. One such excitation can be caused by gamma radiation. Germanium is a semiconductor with a band gap of 0.67 eV. The number of electron-hole pairs is proportional to the energy of the absorbed high-energy photons enabling us to measure the energy of the gamma emission.

Practical Remarks

Due to the very low band gap energy, the germanium must be cooled down using liquid nitrogen, or an electromechanical cooler. Additionally the device used in this experiment is very expensive and fragile, additional care should be taken to prevent damage in fragile arrays such as the connected part between the detector and the lead chamber.

Radioactive Activity

We want to make an estimation of activity of different samples, this quantifies how radioactive a sample is, and thereby its potential hazard. To do this we must relate parameters of time, solid angle and detection rate as in the formula:

$$A = \frac{N}{t \cdot \frac{\Omega}{4\pi} \cdot \epsilon(E_\gamma) \cdot \Gamma(E_\gamma) \cdot \omega(E_\gamma)} \tag{5}$$

Where Ω is the solid angle of the detector, $\varepsilon(E_\gamma)$ is the detector efficiency, $\Gamma(E_\gamma)$ is the absorption probably of gamma radiation and $\omega(E_\gamma)$ is the emission probability.

Experiment

The scintillation detector and semiconductor detector both had lead containers feeding into them, where the radioactive source would be held during measurement periods. Putting the gamma emitting sources into the lead containers minimized the exposure of the experimenter to radiation.
The scintillation detector was held at a current of 2.5 A. Turning on the high voltage, we slowly set the voltage of the photomultiplier to 1kV. From there, we're able to use

	a	b	c	d	RMSE
Scintillation	-1.9380×10^{-9}	1.6680×10^{-5}	0.3524	-6.8564	0.0789
Semiconductor	7.0972×10^{-10}	-3.5781×10^{-6}	0.2062	1.8323	0.0169

Table 1: Root-Mean-Square error and Polynomial fit coefficients for scintillation and semiconductor detectors

software to record the readings.
The semiconductor detector was to be connected to an electronic cryostat to keep the germanium's short band gap from being excited due to room temperature. We establish an electric field on electrodes to capture electrons and holes, to do this we again, turn on the power supply, and slowly apply a 4kV voltage across the electrodes.

Calibration

The calibration of the two devices was done with two elements with known energy spectra. Firstly, Cs-137 gives us a clear energy peak for photons of energy 662 ± 0.5 keV, Eu-152 gives us 3 additional peaks, which we can identify as 121 ± 0.5 keV, 244 ± 0.5 keV and 344 ± 0.5 keV.[8] We calibrate the device's readings to these points and fit a 3rd degree polynomial. Idealy, the calibration curve should be a straight line (1st degree polynomial), but we overfit to a 3rd order to notice if there are too-strong deviations from this expected behaviour. We define the residual as the 2nd and 3rd power term:

$$R_i = (ax_i^3 + bx_i^2 + cx_i + d) - (cx_i + d) = ax_i^3 + bx_i^2$$

Then taking the root-mean-square error, we quantify the quality of the fit. Letting N be the amount of bins:

$$\text{RMSE} = \sqrt{\frac{1}{N}\sum_{i=1}^{N} R_i^2} = \sqrt{\frac{1}{N}\sum_{i=1}^{N}(ax_i^3 + bx_i^2)^2}$$

The fits and errors of the two instruments are summarized in Table 1 and a comparison of the 3rd degree calibration curve is visualized in Figure 3.

Execution

After the calibration we identify the spectra of the elements: Bismuth-207, Cobalt-60, Sodium-22, Europium-152, Cesium-137 and two unknown mixtures A and B. This is done by simply putting the respective sources into the lead casings and recording a reasonable time for photo-peaks to be identified.

Estimation of Source Activity

We want to make a general estimation of the activity by counting how many gamma rays are released into the solid angle of a rate-meter from the radioactive source Cs-137. We do this measuring the readings at different positions $(10 \pm 0.5cm, 20 \pm 0.5cm, 30 \pm 0.5cm, 40 \pm 0.5cm, 50 \pm 0.5cm)$ from the source. A diagram of the experiment is found in 4. Here the opening of the source is the origin and $\vec{r}$ is the position of the infinitesimal surface element, $\hat{n}$ is the unit vector on the solid angle's surface and $\hat{r} = \frac{\vec{r}}{r}$. D is the distance of the source to the disc detector on the rate-meter, R is the distance from the source to the edge of the detector. d is the diameter of the disc.

Our rate-meter has a disk-like detection area which isn't identical to any solid-angle form. Therefore we have to approximate that the area of the disk of diameter d is similar

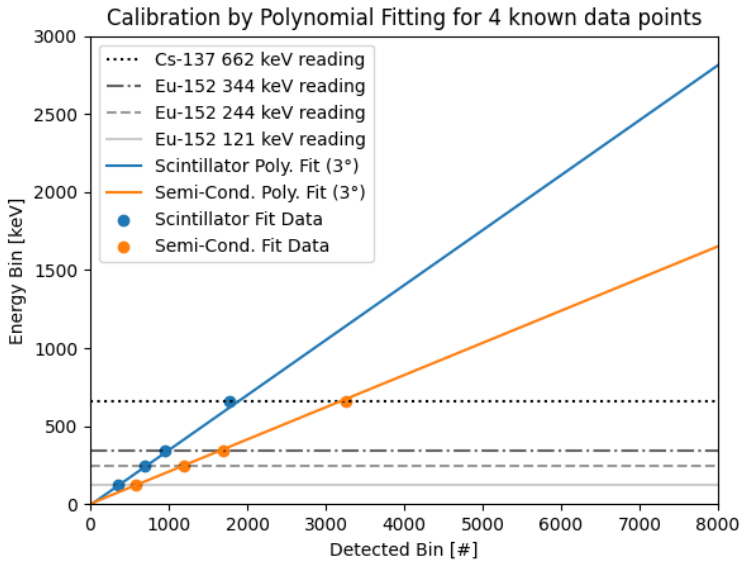

Figure 3: Comparison of the 3rd degree polynomial calibration fit for Eu-152 and Cs-137 energy values on both instruments.

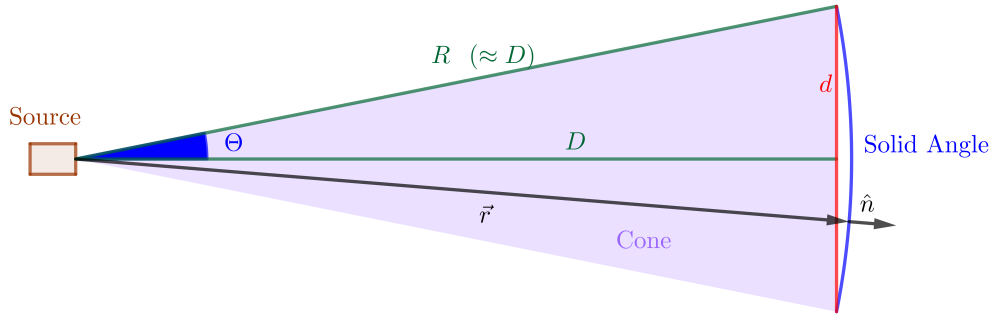

Figure 4: Geometrical Diagram of the Rate-Meter Experiment

to that of a solid angle. This approximation is best for $\tan(\theta) = d/D \ll 1$, and we make the assumption that this error is negligible. The solid angle is defined as:

$$\Omega = \iint_S \frac{\hat{r} \cdot \hat{n}}{r^2} dS \tag{6}$$

We note that $\hat{r} || \hat{n}$ meaning $\hat{r} \cdot \hat{n} = 1$.

$$\Omega = \iint_S \frac{\hat{r} \cdot \hat{n}}{r^2} dS = \int_0^{2\pi} \int_0^{\Theta} \frac{\hat{r} \cdot \hat{n}}{r^2} r^2 \sin(\theta) d\theta d\phi = 2\pi(1 - \cos(\Theta))$$

Where $\Theta = \arctan(\frac{d/2}{D})$ so:

$$\Omega(D) = 2\pi\left(1 - \cos\left(\arctan\left(\frac{d/2}{D}\right)\right)\right) = 2\pi\left(1 - \frac{1}{\sqrt{1 + (\frac{d}{2D})^2}}\right)$$

We then want to fit the readings to the function $f = \frac{c}{x^2} + b$ where we find the best fit c nad b[9]. We expect f to be of this form because we're measuring how the area increase decreases the activity. This form matches the expected units.

Activity Equation: Scintillation Detector

To find the activity, we refer to 5. For the product, $\Omega \cdot \varepsilon$ we consider the integrals:

$$\Omega\varepsilon = \frac{2\pi}{a_0^2}\int_0^{r_0} r \cdot (1 - \exp(-\mu_1 \cdot s_0)) \cdot dr \tag{7}$$

$$\Omega\varepsilon = \frac{2\pi}{a_0^2}\int_{r_0}^{r_d} r \cdot (1 - \exp(-\mu_1(E) \cdot s_1)) \cdot \exp(-\mu_2(E) \cdot s_2) \cdot dr \tag{8}$$

These equations represent two forms of absorption, one either going directly into the detector, the other firstly passing through some lead. Summing them up gives us our wanted quantity $\Omega\varepsilon$. We define s_1, s_2 and s_2 as the vertical distance of intersection of incident gamma waves with the detector, defined as r in Figure 5.

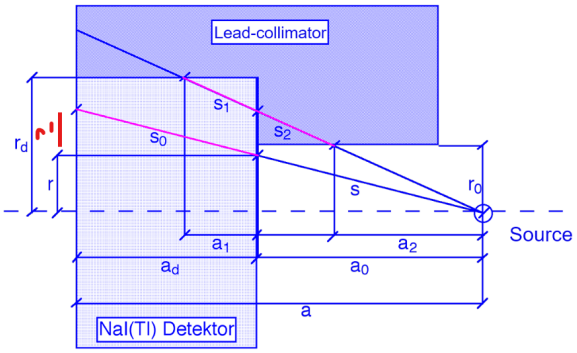

Figure 5: A figure showing the two possible paths a gamma ray can take in the scintillation detector. Note that the given r only relates to the path given below where the gamma ray doesn't enter the lead-collimator

Using the fact that triangle $\Delta(r', s_0, a_d)$ and $\Delta(r, s, a_0)$ are congruent, we get 10

$$r' = \frac{a_d}{a_0} \cdot r \tag{9}$$

$$s_0^2 = r'^2 + a_d^2 = \left(\frac{a_d}{a_0} \cdot r\right)^2 + a_d^2 \tag{10}$$

For the other case, we use the congruency of $\Delta(r, a_0, s_2 + s) \approx \Delta(r_0, a_2, s)$ and $\Delta(r_d - r, a_1, s_1 + s) \approx \Delta(r - r_0, a0 - a_2, s_2)$ and get:

[9] b refers to the background radiation.

$$\frac{s_1}{s_2} = \frac{r_d - r}{r - r_0} \tag{11}$$

$$a_2 = \frac{r_0}{r} \cdot a_0 \tag{12}$$

$$s_2^2 = (r - r_0)^2 + (1 - \frac{r_0}{r})^2 \cdot a_0^2 \tag{13}$$

With these functions, we can numerically integrate 7 and 8 to use for the definition of activity of a source. The values used for the mass attenuation and the calculated $\Omega \cdot \varepsilon$ are summarized in Table 2.

Table 2: Mass attenuation values and $\Omega \cdot \varepsilon$ functions

Index	**Mass attenuation**	$\Omega \cdot \varepsilon$ **(no lead)**	$\Omega \cdot \varepsilon$ **(with lead)**
1	0.28259	0.25645654	0.01231880
2	0.51013	0.25645654	0.00733602
3	0.18350	0.25645654	0.01714770
4	0.20919	0.25645654	0.01578217
5	0.18717	0.25645654	0.01683841

Activity Equation: Semiconductor Detector

Here we can follow the same principles as we did before in finding A for the scintillation detectors, but we don't have certain parameters. We define:

$$F(E_\gamma) = \frac{\Omega}{4\pi} \cdot \epsilon(E_\gamma) \cdot \Gamma(E_\gamma) \tag{14}$$

We want the fit to have the form $C_0 e^{b \cdot E_\gamma}$. Knowing that the Europium sample has the activity of 8350 Bq and that $F(E_\gamma) = \frac{N}{t \cdot \omega(E_\gamma) \cdot A}$, we fit observed photo-peaks as in 6 to find the values $C_0 = 22$ with uncertainty $\sigma_{C_0} = 1.9$ and $b = -1.4$ with uncertainty $\sigma_b = 0.012$.

Results

The raw data of the readings are found in Figure 9 for the scintillation detector and Figure 10 for the semiconductor detector. From this raw data we notice key features of the behaviour of gamma-radiation interactions.

Gaussian Fit of Photo-Peaks

The raw data in the appendix also provides windows where Gaussian fits were taken of characteristic photo-peaks. The standard deviation depicts the statistical error of the detectors and characterizes their effectiveness. Additionally, the resolution, given as:

$$R = \frac{\Delta E}{E} \tag{15}$$

Where ΔE = FWHM is the Full-Width-at-Half-Maximum. This quantifies how far apart two photo peaks have to be in order to be distinguishable. The lower R is, the

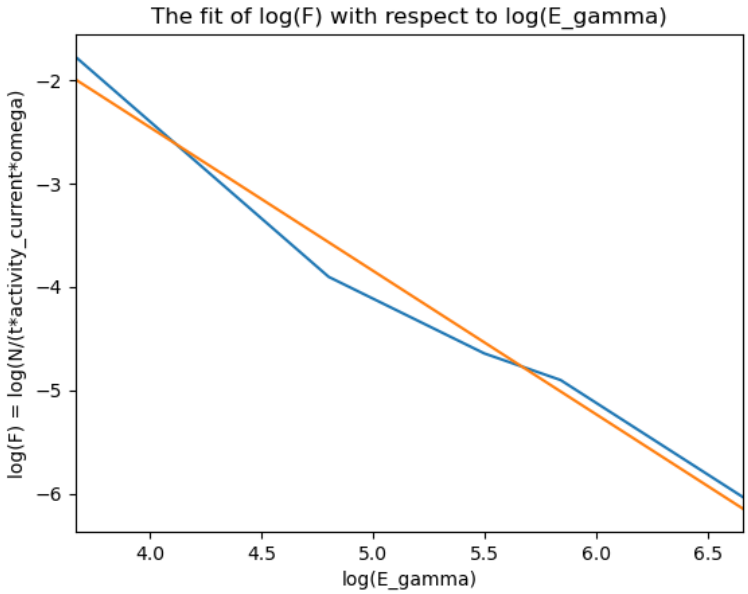

Figure 6: The fit of the $F(E)$ function in the linear log/log representation.

Table 3: Photo-peaks and resolution measurements from the scintillation detector.

Element	**Energy (keV)**	**Standard Deviation (keV)**	**Resolution**
Bi-207	558.20	17.31	0.07301
Co-60	1212.14	20.84	0.04048
Na-22	512.32	19.75	0.09079
Eu-152	343.63	13.45	0.09215
Cs-137	660.86	18.71	0.06668
Mixture A (8)	658.04	20.43	0.07311
Mixture B (9)	660.09	20.59	0.07346

better the resolution of the instrument. We summarize the results of the two detectors in Table 3 and 4.

We also want to analyse if the spectrum has attributes of Poisson statistics. For this, we make an analysis of the energy-resolution relation (Figure 11a and 12a) and the energy-variance relation (Figure 11b and 12b). For a Poisson distribution, we expect that Var(X) = E(X) so we additionally do a linear fit.[10] The results are summarized in Table 5, due to the seeming presence over outlier we omit it for the linear fit for both cases.

Source Activity

First estimation

For the rate-meter readings, we get the fit of Figure 7. The results are summarized in 6.

The fit ends up with $c = 109121.57 \pm 136.06$ and $b = -26.221 \pm 0.814$.

[10] X here is simply a Poisson random variable.

Table 4: Photo-peaks and resolution measurements from the semiconductor (Germanium) detector.

Element	**Energy (keV)**	**Standard Deviation (keV)**	**Resolution**
Bi-207	568.96	0.61	0.00254
Co-60	1404.00	1.00	0.00168
Na-22	510.12	1.22	0.00564
Eu-152	344.01	0.51	0.00347
Cs-137	662.01	0.62	0.00221
Mix. A (8)	662.11	0.66	0.00235
Mix. B (9)	662.08	0.66	0.00233

Table 5: Linear fit parameters and R^2 values for Poisson analysis of the detectors.

Detector	**Slope** a	**Intercept** b	R^2
Scintillation	1.1516	169.7235	0.7173
Germanium	1341.2484	70.1909	0.9831

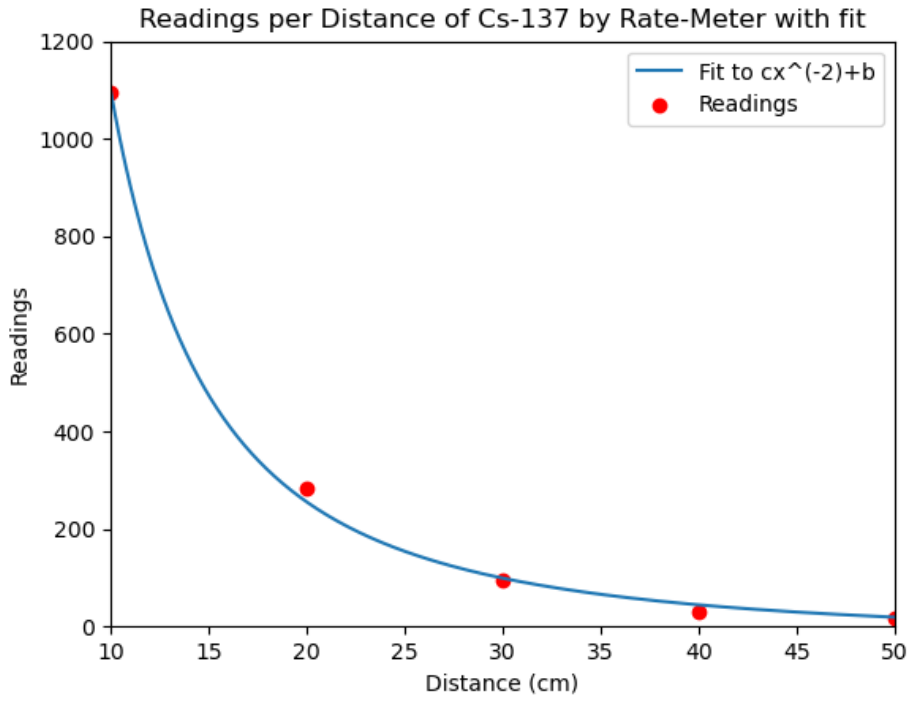

Figure 7: Readings and Distance relation of Cs-137 by rate-meter

Activity of different Sources

The activity due to the scintillation detector and the semiconductor detector is summarized in Table 7.

Distance (cm)	Counts	Counts per Solid Angle
$10 \pm \sqrt{2}$	1095 ± 0.5	11641.96 ± 3045.82
$20 \pm \sqrt{2}$	284 ± 0.5	11875.10 ± 1323.25
$30 \pm \sqrt{2}$	94 ± 0.5	8815.58 ± 315.72
$40 \pm \sqrt{2}$	29 ± 0.5	4829.64 ± 371.91
$50 \pm \sqrt{2}$	16 ± 0.5	4161.34 ± 658.27

Table 6: Measured counts and counts per solid angle at various distances.

Table 7: Measured activities of the isotopes using both the scintillation and semiconductor (Germanium) detectors.

Isotope	Scintillation Activity (Bq)	Semiconductor Activity (Bq)
Cs	13400 ± 804	36100 ± 492
Eu	5700 ± 1200	–
Co	61 ± 4	3400 ± 92
Bi	650 ± 56	26000 ± 4522
Na	4.4 ± 0.2	94 ± 9.4
Mix A	44000 ± 2620	23000 ± 15306
Mix B	30000 ± 1840	17000 ± 11207

Discussion

From the calibration results, we can already see a performance difference between the two detection instruments. Firstly, the third and second order term is smaller for the semiconductor, meaning it's non-linear properties are weaker. Additionally, the intercept of the y-axis is closer to 0 with the semiconductor, supporting the fact that we expect no energy readings of 0 energy. Lastly, the Root-Mean-Square error is smaller for the semiconductor detector. This means the average of the square error is much smaller for each point of a linear fit than for the third degree polynomial. In conclusion, The calibration has better properties with the semiconductor detector than with the scintillation detector.
Nonetheless, for both detectors, the core reason for a non-linearity could be attributed to the Cs-137 reading of 662 keV energy. In Figure 3 this energy level strays slightly from the fit curve in both detectors. A potential reason for this would that the conditions of detection get altered when changing the samples, a potentially problematic systematic error in the experiment. A good way to avoid this problem would be to calibrate the system according to features of an element, and then use that calibration on that element alone, this requires a lot of prior information to be known which isn't always possible. Another way is to make the procedure of changing sources more controlled and less prone to potential systemic errors. A more elaborate casing would prevent background radiation from sporadically affecting the sensor.

Graphical Analysis

Since the scintillation detector has a weaker resolution, its photo-peaks are less protruding and lets us graphically analyse the behaviour of the photon-electron interactions clearer. The clearest element for this analysis appears to be cesium. In Figure 8 we see a more focused render of the data on the range of interest. We note two x-ray emissions, one from the lead and another from the barium meta-state. The barium x-ray can occur when the energy of a photon excites the 1s atomic shell which is then substituted for an electron in a higher shell.[5] For this to happen, the electron must release energy

in the form of x-ray radiation. Theoretically, this happens at 32.19 keV[11] and Figure 8 shows a reasonable correspondence to this peak, but the peak does not match fully experimentally. Lead x-rays are due to the photoelectric effect, as lead has a characteristically high density of electrons[12]. This peak is theoretically set at 75 keV which is poorly matched in our raw data depiction.[6]
The Compton continuum sits between the backscatter peak and the Compton edge. This is due to the mechanical nature of Compton scattering, where energy is determined by the incidence of the photon-electron interaction, thereby letting the energy take on a uniformly distributed range.
The backscatter peak occurs due to the strong reflection angle of Compton scattering at $\theta = \pi$ in 3. Since the electron moves towards the source, although the photon loses maximal energy, it reflects sharply towards the detector, causing a small peak. Inserting $\theta = \pi$ into 3 gives a backscatter approximation at 184 keV, which doesn't match well to the graph's prediction. The Compton edge occurs due to the opposite effect where $\theta = 0$, causing the photon to reflect back towards the source, closing the continuum.[7]

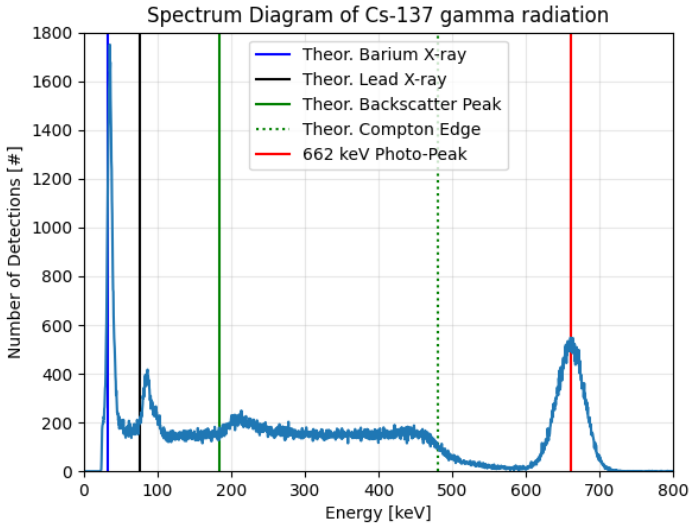

Figure 8: ^{137}Cs Graphical Analysis with annotated Theoretical Values

Comparison of Photo-peak Detection

Comparing Table 3 and 4 we see that the semiconductor resolution has strikingly better results. The standard deviation and the resolution are an entire order lower, meaning the semiconductor is generally more precise, implying a smaller statistical error with the semiconductor detector.
There seems to be an anomaly with the Cobalt-60 measurement. The shift in the energy level by 200 keV higher sits outside the range of the standard deviations. Also, graphically in Figure 9 and 10 we see that the two protruding photo-peaks are shifted to the right. This implies that a systematic error in the calibration. Seeing how the calibration between the two detectors is different and the Cobalt-60 is the only element

[11] 32.19keV is the difference between 661.9keV-625.67keV where 661.9keV is an outer electron that produces the X-ray and 625.67 is the energy of the 1s electron that escaped.
[12] Also thereby making it a good shield for gamma radiation (high probability of photon-electron interaction)

that reaches keV above 1200 for its photo-peak and the calibration is done with energy levels between 121-662 keV, it is expected that for values further away from this range, inaccuracies will occur. Therefore, we make the conclusion that the photo-peak of the semiconductor detector is probably more accurate (without looking at the theoretical value) due to its better calibration parameters.
Our attempt at the Poisson analysis seems to be most promising with the scintillation detector, where the slope is the closest to 1. The germanium is off by multiple order but expresses a better linear fit due to having a higher R^2 value. Otherwise, the fact that we remove and outlier for the linear fit gives less weight to this analysis. A repetition would solidify the conclusion
A way to improve this measurement is to have a calibration result with higher energy, this would further strengthen the accuracy of the device, and give a more consistent result between the two detectors.

Source Activity

For the first estimation, where the counts are measured at different distances from the source Cs-137, we see in Figure 7 that the fit for the detection has a similar form to the expected readings, but it doesn't match perfectly. Despite the low expected statistical error, there seems to be another term missing in the fit function that adjusts for this behaviour. Looking at the counts per solid angle, we see that the error decreases with distance, and the change in the error comes purely due to the solid angle component. The decrease in error with distance is due to there being less counts at larger distance. One error that isn't quantified is the approximation of the rate-meter disk detector as a solid angle. This would also imply a larger error as the distance increases, since the approximation is more accurate when $\frac{d}{D} \ll 1$.
An improvement to this part of the experiment would be quantifying this systematic flaw, or using detectors that somehow adapt to a solid angle form. Additionally, doing the experiment multiple times and taking the average values for each data point would further solidify the result.

Different Sources

In general the results found were quite sporadic, we see a general lack of consistency, and no admissible conclusion can be made regarding either the activity values, or the comparison between the detector activity. No two values of the detectors sit within the standard deviation range, despite it being absurdly high at times. The randomness can note towards a massive statistical error that has a strong effect on the results. Therefore, the question of precision and consistency would be the first to be pursued in another attempt at the experiment. Perhaps in order to improve this experiment, it would have been smarter to compare some more theoretical values and see whether this is a statistical or systematic error. This would help point towards the issue of either the calculations, method or the device itself.

Mixture A and Mixture B

In order to identify the elements of Mixture A and Mixture B, we turn to the higher resolution data of the semiconductor. In Figure 10 it's hard to conclude the presence of any other element but the Cs-137 isotope.

Conclusion

In general, we've been able to clearly identify differences between the two detectors in their effectiveness of detecting the gamma-ray spectrum of various sources.In the calibration, we've seen that the semiconductor detector was clearly better at fulfilling our assumption of having a linear calibration curve. The lower resolution pointed towards a better precision in energy photo-peak identification.
Graphical analysis of cesium was, on the other hand, better done with the scintillation detector, certain attributes would be clearer to see, such as the Compton spectrum and the x-rays of led, as well as the photo-peak. Despite this, theoretical values for these attributes were off by quite a lot meaning potential problems with calibration. It should be noted that calibration would've been more accurate if we made these matches with the theoretical values.
As to the photo-peak detection of the different materials, we again observe that the semiconductor consistently identifies these parameters with high precision, but an anomaly with the cobalt peak implies a systematic inaccuracy of the calibration at higher energies (they are further away from the calibration values).
Looking at the emission rates relative to the distance of the rate-meter, we see a relatively good fit, but one that could benefit from repeated measurement.
For the activity reading, we found extremely random behaviour, pointing towards a strong statistical error. Not much can be said on the data other than the fact that the experiment yielded poor results for this parameter.
In conclusion, this experiment did successfully compare the two detectors, and went into depth of their workings. The semiconductor experiment, making use of germanium's small band gap, was significantly better than the scintillation detector at detecting photo-peaks. The radioactive activity measurement unfortunately didn't help at all, and revisions of the experiment in that part would be ideal.

Appendix

This report benefitted from ChatGPT and DeepSeek for LaTeX table formatting and python syntax recollection.

References

[1] Wikipedia.
Gamma ray.
`https://en.wikipedia.org/wiki/Gamma_ray`

[2] Wikipedia.
Cobalt-60 Decay Scheme (Image).
`https://en.wikipedia.org/wiki/Gamma_ray#/media/File:Cobalt-60_Decay_Scheme.svg`

[3] Wikipedia.
Caesium-137.
`https://en.wikipedia.org/wiki/Caesium-137`

[4] Maximus Energy.
The Rich Physics of Cs-137 Gamma Spectrum.
`https://maximus.energy/index.php/2020/10/24/the-rich-physics-of-cs-137-gamma-spectrum/?srsltid=AfmBOoqdXKMz26cpdB6Tci4WA_BTLSX5wRd_MueczaPp75jvAjHLpyH8`

[5] LD Didactic.
Appendix: Cs-137.
https://www.ld-didactic.de/software/524221en/Content/Appendix/Cs137.htm

[6] U.S. Nuclear Regulatory Commission (NRC).
Background on Cesium-137.
https://www.nrc.gov/docs/ml1122/ml11229a703.pdf

[7] National Institute of Standards and Technology (NIST).
Gamma-Ray Measurements and Standards.
https://nvlpubs.nist.gov/nistpubs/jres/123/jres.123.012.pdf

[8] ETH Zurich.
Gamma Ray Spectroscopy Manual.
https://p3p4.phys.ethz.ch/manuals/Gamma_Ray_Spectroscopy.pdf

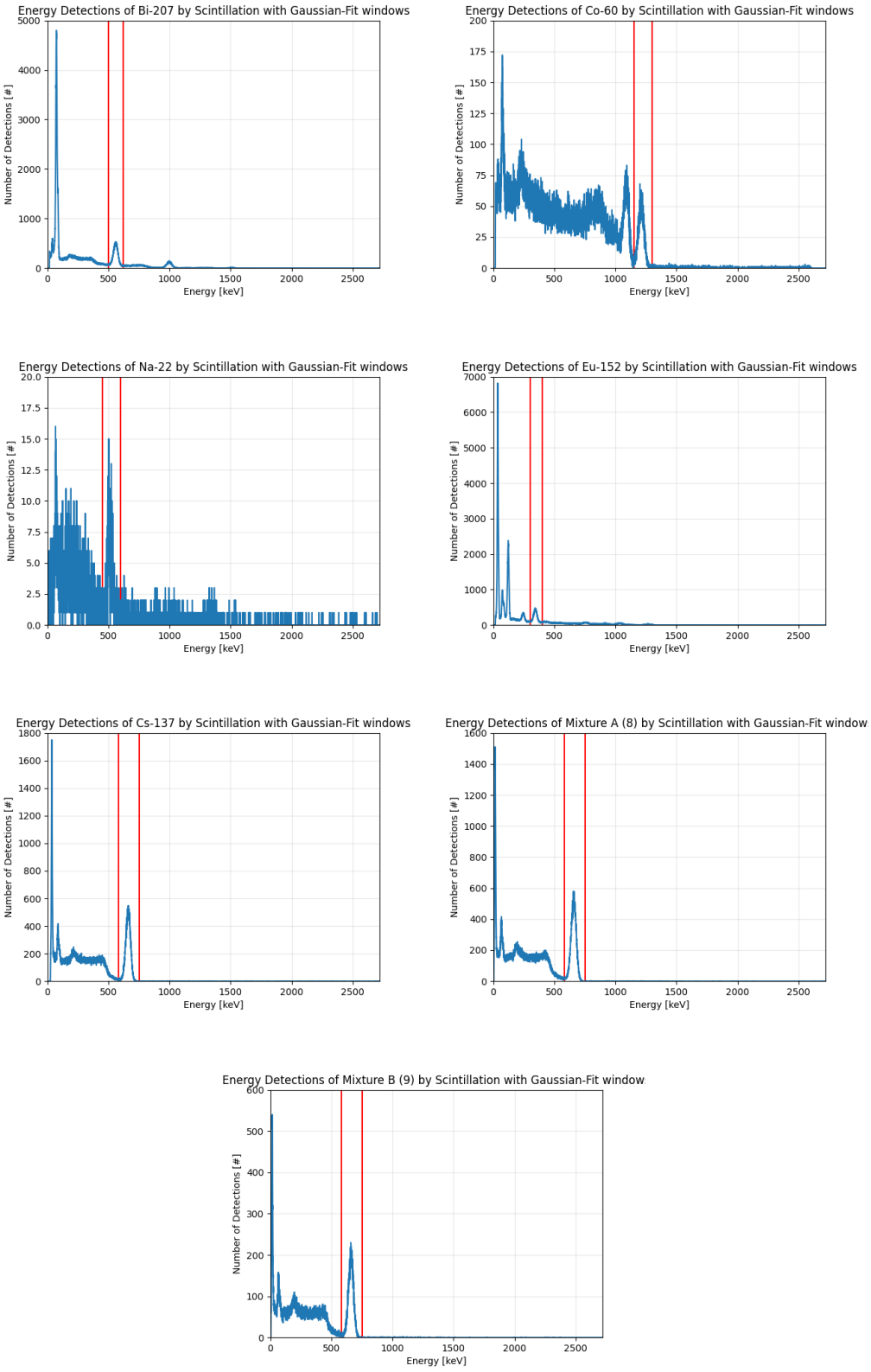

Figure 9: The raw data of the scintillation device for elements (from left to right) Billirium-207, Cobalt-60, Sodium-22, Europium-152, Cesium-137, Mixture A, Mixture B

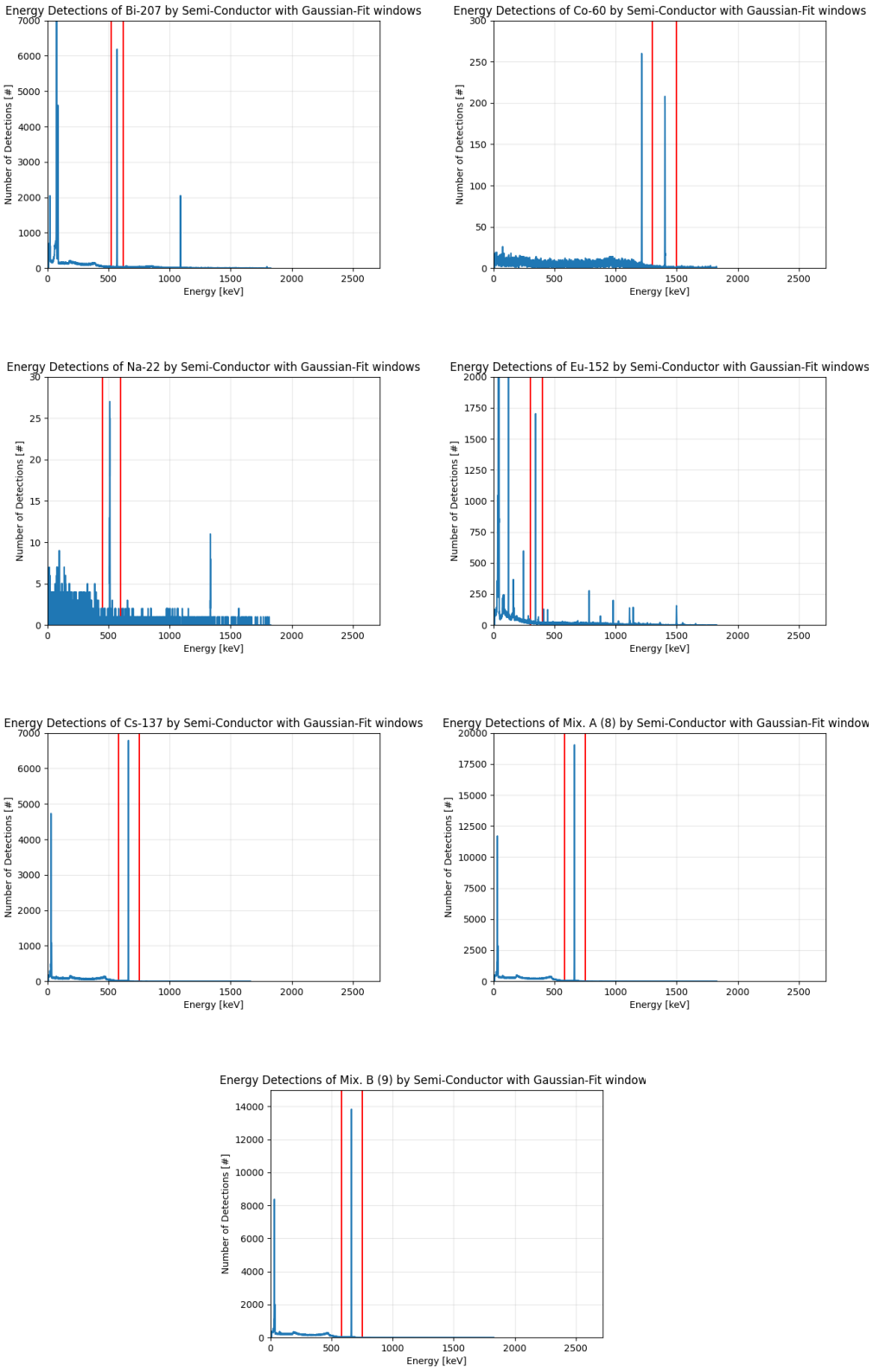

Figure 10: The raw data of the Semiconductor detector for elements (from left to right) Bismuth-207, Cobalt-60, Sodium-22, Europium-152, Cesium-137, Mixture A, Mixture B

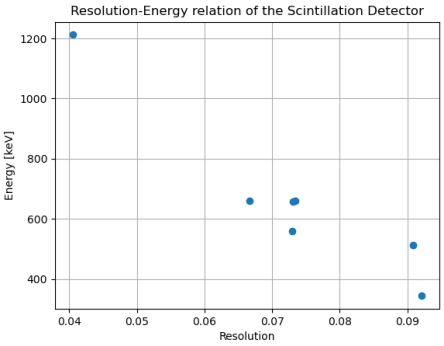

(a) Resolution vs Energy (Scintillator)

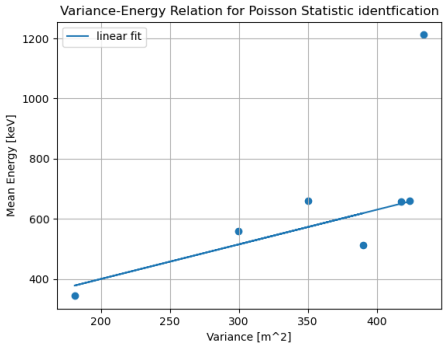

(b) Variance vs Energy (Scintillator)

Figure 11: Poisson analysis of the scintillation detector.

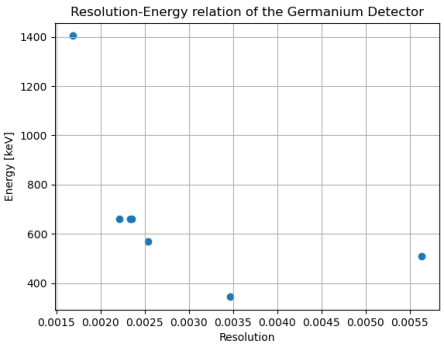

(a) Resolution vs Energy (Germanium)

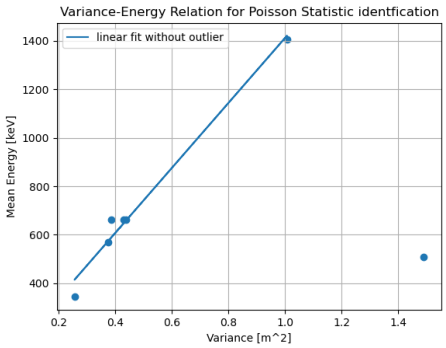

(b) Variance vs Energy (Germanium)

Figure 12: Poisson analysis of the germanium detector.